Triple photonic band-gap structure dynamically induced in the presence of spontaneously generated coherence

Jin-Wei Gao, Qian-Qian Bao, Ren-Gang Wan, Cui-Li Cui,[*] and Jin-Hui Wu[†]

College of Physics, Jilin University, Changchun 130012, People's Republic of China

We study a cold atomic sample coherently driven into the five-level triple-Λ configuration for attaining a dynamically controlled triple photonic band-gap structure. Our numerical calculations show that three photonic band gaps with homogeneous reflectivities up to 92% can be induced on demand around the probe resonance by a standing-wave driving field in the presence of spontaneously generated coherence. All these photonic band gaps are severely malformed with probe reflectivities declining rapidly to very low values when spontaneously generated coherence is gradually weakened. The triple photonic band-gap structure can also be attained in a five-level chain-Λ system of cold atoms in the absence of spontaneously generated coherence, which however requires two additional traveling-wave fields to couple relevant levels.

I. INTRODUCTION

Laser-induced atomic coherence has been extensively studied during the past few decades and has led to the reports of many interesting effects such as electromagnetically induced transparency (EIT) [1], lasing without population inversion (LWI) [2], stimulated Raman adiabatic passage (STIRAP) [3], and quantum memory of photonic states [4]. Recently, to achieve the efficient control and flexible manipulation of light propagation, laser-induced atomic coherence has been extended from the spatially homogeneous pattern into the spatially periodic pattern so that stationary light pulses (SLPs) [5–11] and dynamic photonic band gaps (D-PBGs) [12–17] are theoretically foreseen and experimentally observed. The essence of such an extension relies on the application of at least one standing-wave (SW) driving field on a cold or thermal atomic sample with suitable energy levels. In the presence of a SW potential, a forward (FW) propagating probe field may be transformed into a backward (BW) propagating probe field due to the photonic Bragg scattering with a good transparency background (cf. D-PBGs), and a wave packet of spin coherence may be transformed into a light pulse with a zero group velocity due to the balanced nonlinear mixing between FW and BW photons (cf. SLPs). D-PBGs and SLPs have been exploited to design new schemes for all-optical routing, switching, and confinement [18–21] of weak light signals, which are important in quantum information processing.

So far all investigations on D-PBGs have been restricted to the controlled generation and potential application of one or two band gaps around an atomic resonance [12–17]. In this paper we will demonstrate a feasible scheme for the simultaneous generation of three or even more band gaps with the purpose of further improving light-processing capabilities in actual situations. This scheme depends on the existence of three or even more closely lying nonorthogonal excited levels exhibiting the maximal spontaneously generated coherence (SGC) when atoms decay from them to a common ground level. SGC refers to in fact the vacuum-induced quantum interference between indistinguishable spontaneous decay channels and has been well studied to achieve spontaneous emission suppression [22], two-photon correlation [23], coherent population transfer [24], etc. In particular, it has been found that SGC can be enhanced in left-handed materials [25] or plasmonic nanostructures [26] and may be modified by dynamic energy shifts when counterrotating terms are included in the Hamiltonian [27].

We study here a five-level triple-Λ system [28,29] interacting with a weak probe field and a strong driving field and exhibiting the maximal SGC on both probe transitions and driving transitions. SGC first provides for the probe field an ideal absorption background with two space-independent transparency windows, which are then split into three space-sensitive transparency windows by the driving field set in the SW pattern. Since the refractive index changes periodically in space like the absorption coefficient, three D-PBGs are expected to arise in these transparency windows due to nearly perfect photonic Bragg scattering accompanied by negligible absorption. This expectation is confirmed by a few numerical plots, from which we can see a triple D-PBG structure manifested by probe reflectivities of up to 92% in three different spectral regions. The triple D-PBG structure can also be attained in a five-level chain-Λ system without SGC in that it is equivalent to a five-level triple-Λ system with SGC in the dressed state representation of two additional traveling-wave (TW) coupling fields. Finally we stress that more D-PBGs may be simultaneously generated around the probe resonance when a five-level triple-Λ (chain-Λ) system is extended into an *m*-level multi-Λ (chain-Λ) system with $m = 7, 9, 11, \ldots$.

II. MODEL AND EQUATIONS

We consider in Fig. 1 a five-level atomic system with two far-spaced lower levels $|0\rangle$ and $|4\rangle$ and three closely lying upper levels $|1\rangle$, $|2\rangle$, and $|3\rangle$. A weak probe field $\vec{E}_p$ and ω_p couples level $|0\rangle$ to the three upper levels with Rabi frequencies $\Omega_{pi} = \vec{E}_p \cdot \vec{d}_{i0}/2\hbar$ while a strong driving filed $\vec{E}_s$ and ω_s couples level $|4\rangle$ to the three upper levels with Rabi frequencies $\Omega_{si} = \vec{E}_s \cdot \vec{d}_{i4}/2\hbar$ where $\vec{d}_{ij}$ is the

---

*cuicuili@jlu.edu.cn

†jhwu@jlu.edu.cn
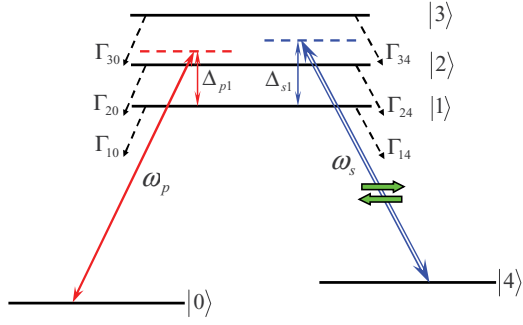
FIG. 1. (Color online) Schematic of a five-level triple-Λ system having two far-spaced lower levels and three closely lying upper levels. A weak traveling-wave field ω_p probes all transitions from the triplet to level $|0\rangle$ while a strong standing-wave field ω_s drives all transitions from the triplet to level $|4\rangle$.

dipole moment on transition $|i\rangle \leftrightarrow |j\rangle$. The probe (driving) field ω_p (ω_s) is assumed to be detuned from transitions $|i\rangle \leftrightarrow |0\rangle$ ($|i\rangle \leftrightarrow |4\rangle$) by $\Delta_{pi} = \omega_{i0} - \omega_p$ ($\Delta_{si} = \omega_{i4} - \omega_s$). The probe and coupling detunings may also be expressed as $\Delta_{p2} = \Delta_{p1} + \omega_{21}$, $\Delta_{p3} = \Delta_{p1} + \omega_{31}$, $\Delta_{s2} = \Delta_{s1} + \omega_{21}$, and $\Delta_{s3} = \Delta_{s1} + \omega_{31}$ when frequency separations ω_{21} and ω_{31} are relatively small. The spontaneous decay rates from the upper levels to the lower levels are denoted by Γ_{ij} with $i = 1,2,3$ and $j = 0,4$.

Under the electric-dipole and rotating-wave approximations, the interaction Hamiltonian for the atom+field system under consideration can be written as

$$H = \hbar \begin{pmatrix} 0 & \Omega_{p1}^* & \Omega_{p2}^* & \Omega_{p3}^* & 0 \\ \Omega_{p1} & \Delta_{p1} & 0 & 0 & \Omega_{s1} \\ \Omega_{p2} & 0 & \Delta_{p2} & 0 & \Omega_{s2} \\ \Omega_{p3} & 0 & 0 & \Delta_{p3} & \Omega_{s3} \\ 0 & \Omega_{s1}^* & \Omega_{s2}^* & \Omega_{s3}^* & \Delta_{p1} - \Delta_{s1} \end{pmatrix}, \quad (1)$$

from which it is straightforward to attain 25 dynamic equations for the mutually coupled density matrix elements ρ_{ij} with $i,j \in \{0,1,2,3,4\}$.

In the weak probe limit, we are allowed to further set $\rho_{00} = 1$ and $\rho_{11} = \rho_{22} = \rho_{33} = \rho_{44} = 0$ so that the 25 density matrix equations reduce to

$$\begin{aligned} \partial_t \rho_{10} &= -(\gamma_{10} + i\Delta_{p1})\rho_{10} + i\Omega_{p1} + i\Omega_{s1}\rho_{40} \\ &\quad - \gamma_{12}\rho_{20} - \gamma_{13}\rho_{30}, \\ \partial_t \rho_{20} &= -(\gamma_{20} + i\Delta_{p2})\rho_{20} + i\Omega_{p2} + i\Omega_{s2}\rho_{40} \\ &\quad - \gamma_{12}\rho_{10} - \gamma_{23}\rho_{30}, \\ \partial_t \rho_{30} &= -(\gamma_{30} + i\Delta_{p3})\rho_{30} + i\Omega_{p3} + i\Omega_{s3}\rho_{40} \\ &\quad - \gamma_{23}\rho_{20} - \gamma_{13}\rho_{10}, \\ \partial_t \rho_{40} &= -(\gamma_{40} + i\Delta_{p1} - i\Delta_{s1})\rho_{40} + i\Omega_{s1}^*\rho_{10} \\ &\quad + i\Omega_{s2}^*\rho_{20} + i\Omega_{s3}^*\rho_{30}, \end{aligned} \quad (2)$$

where $\gamma_{10} = (\Gamma_{10} + \Gamma_{14})/2$, $\gamma_{20} = (\Gamma_{20} + \Gamma_{24})/2$, $\gamma_{30} = (\Gamma_{30} + \Gamma_{34})/2$, and γ_{40} are the dephasing rates of ρ_{10}, ρ_{20}, ρ_{30}, and ρ_{40}, respectively; $\gamma_{12} = p_{12}\sqrt{\Gamma_{10}\Gamma_{20}}/2 + \tilde{p}_{12}\sqrt{\Gamma_{14}\Gamma_{24}}/2$, $\gamma_{13} = p_{13}\sqrt{\Gamma_{10}\Gamma_{30}}/2 + \tilde{p}_{13}\sqrt{\Gamma_{14}\Gamma_{34}}/2$, and $\gamma_{23} = p_{23}\sqrt{\Gamma_{20}\Gamma_{30}}/2 + \tilde{p}_{23}\sqrt{\Gamma_{24}\Gamma_{34}}/2$ are the cross-coupling

constants between ρ_{10} and ρ_{20}, between ρ_{10} and ρ_{30}, and between ρ_{20} and ρ_{30}, respectively. To be more specific, $p_{ij}\sqrt{\Gamma_{i0}\Gamma_{j0}}/2$ ($\tilde{p}_{ij}\sqrt{\Gamma_{i4}\Gamma_{j4}}/2$) represents the SGC coefficient between indistinguishable decay channels $|i\rangle \rightarrow \|0\rangle$ and $|j\rangle \rightarrow |0\rangle$ ($|i\rangle \rightarrow |4\rangle$ and $|j\rangle \rightarrow |4\rangle$) while $p_{ij} = \vec{d}_{i0} \cdot \vec{d}_{j0}/(|\vec{d}_{i0}||\vec{d}_{j0}|)$ [$\tilde{p}_{ij} = \vec{d}_{i4} \cdot \vec{d}_{j4}/(|\vec{d}_{i4}||\vec{d}_{j4}|)$] denotes the dipole arrangement coefficient for the three probe (driving) transitions. It is clear that $p_{ij} = 0$ ($\tilde{p}_{ij} = 0$) means the vanishing SGC whereas $p_{ij} = \pm 1$ ($\tilde{p}_{ij} = \pm 1$) indicates the maximal SGC between spontaneous decay channels $|i\rangle \rightarrow |0\rangle$ and $|j\rangle \rightarrow |0\rangle$ ($|i\rangle \rightarrow |4\rangle$ and $|j\rangle \rightarrow |4\rangle$). For simplicity, through a specific arrangement of dipole moments and field polarizations, in the following we will set $p_{12} = -p_{13} = -p_{23} = p$ and $\tilde{p}_{12} = -\tilde{p}_{13} = -\tilde{p}_{23} = \tilde{p}$, and $\Omega_{p1} = +\Omega_{p2} = -\Omega_{p3} = \Omega_p$ and $\Omega_{s1} = -\Omega_{s2} = -\Omega_{s3} = \Omega_s$.

Since we are interested in the controlled generation of D-PBGs, the driving field is assumed to be set in the SW pattern so that its Rabi frequency can be expressed as $\Omega_s(z) = 2G_s \cos(k_s z)$ with $k_s = 2\pi/\lambda_s$ being the driving wave vector. Thus we can numerically solve Eqs. (2) to obtain the spatially periodic probe susceptibility

$$\begin{aligned} \chi(\Delta_{p1}, z) = \frac{N}{2\varepsilon_0 \hbar \Omega_p} \big[&d_{10}^2 \rho_{10}(\Delta_{p1}, z) + d_{20}^2 \rho_{20}(\Delta_{p1}, z) \\ &- d_{30}^2 \rho_{30}(\Delta_{p1}, z) \big] \end{aligned} \quad (3)$$

and the spatially periodic refractive index $n(\Delta_{p1}, z) = \sqrt{1 + \chi(\Delta_{p1}, z)}$ of a cold atomic sample with density N and length L. In such atomic samples, a FW propagating probe field may experience nearly perfect photonic Bragg scattering within a certain spectral region and therefore be totally reflected into a BW propagating probe field. To verify this prediction, we utilize the transfer-matrix method to examine the overall optical response of a cold atomic sample described by Eq. (3), in which the light propagation through a single period of length $a = \lambda_s/2$ is governed by a 2×2 unimodular transfer matrix M [30]. Taking into account the translational invariance, we can impose the Bloch condition on M to determine the photonic eigenstates by calculating

$$e^{2i\kappa a} - \text{Tr}(M)e^{i\kappa a} + 1 = 0 \quad (4)$$

with $\kappa = \kappa' + i\kappa''$ being the Bloch wave vector [30]. As is well known, D-PBGs are expected to arise in the frequency regions with $\kappa' = \pi/a$ and $\kappa'' \neq 0$, which is however difficult to check in experiment. An experimentally accessible physical quantity describing D-PBGs is the reflectivity of a probe light incident upon a cold atomic sample of length $L = Ka$ with K being the number of SW periods $a = \lambda_s/2$. Here the probe reflectivity can be written as $|R(\Delta_{p1}, L)|^2$ with

$$R(\Delta_{p1}, L) = \frac{M_{K(12)}(\Delta_{p1}, L)}{M_{K(22)}(\Delta_{p1}, L)} \quad (5)$$

being the reflection amplitude and $M_K = M^K$ the total transfer matrix of the cold atomic sample.

III. RESULTS AND DISCUSSIONS

In Fig. 2(a), both real and imaginary parts of the Bloch wave vector κ are displayed as a function of the probe detuning Δ_{p1} for a series of carefully chosen parameters.
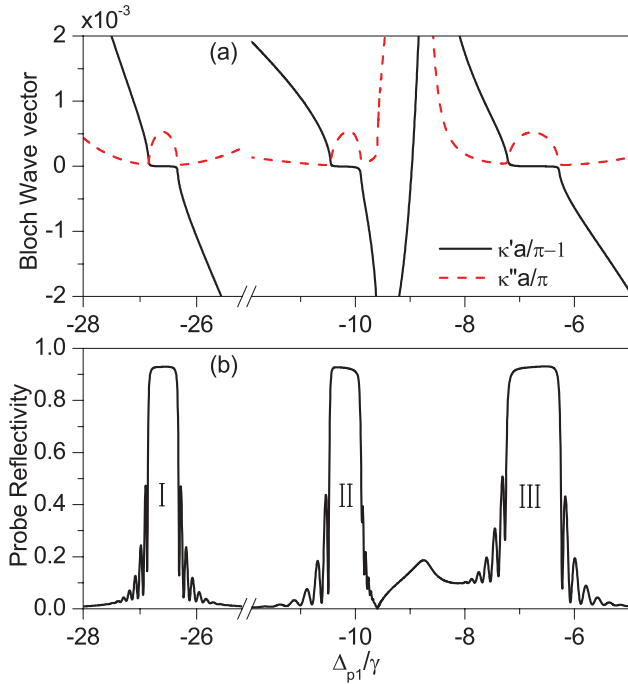
FIG. 2. (Color online) Bloch wave vector $\kappa = \kappa' + i\kappa''$ (a) and probe reflectivity $|R|^2$ (b) versus probe detuning Δ_{p1} with $\tilde{p} = p = 1.0$, $\omega_{21} = 20\gamma$, $\omega_{32} = 12\gamma$, $\Delta_{s1} = -10\gamma$, $\Omega_p = 0.002\gamma$, $G_s = 1.6\gamma$, $\Gamma_{10} = \Gamma_{20} = \Gamma_{30} = \Gamma_{14} = \Gamma_{24} = \Gamma_{34} = \gamma$, $\gamma_{40} = 0.001\gamma$, $\lambda_p = 780.792$ nm, $\lambda_s = 780.778$ nm, $d_{10} = d_{20} = d_{30} = 1.465 \times 10^{-29}$ C m, $N = 1.0 \times 10^{12}$ cm^{-3}, $L = 1.5$ mm, and $\gamma = 6.0$ MHz.

As we can see three D-PBGs open up in different frequency regions around the probe resonance, in which we have nearly perfect photonic Bragg scattering as indicated by $\kappa' = \pi/a$ and $\kappa'' \neq 0$. In Fig. 2(b), the probe reflectivity $|R|^2$ is displayed as a function of the probe detuning Δ_{p1} for the same parameters as in Fig. 2(a). Three rather high platforms (up to 92%) are clearly observed in Fig. 2(b), which once again confirms the ideal development of three D-PBGs. The underlying physics lies in the periodically modulated refractive index $n(\Delta_{p1}, z)$ within several transparency windows of widths and depths quite different at the SW nodes and antinodes. In Fig. 3,
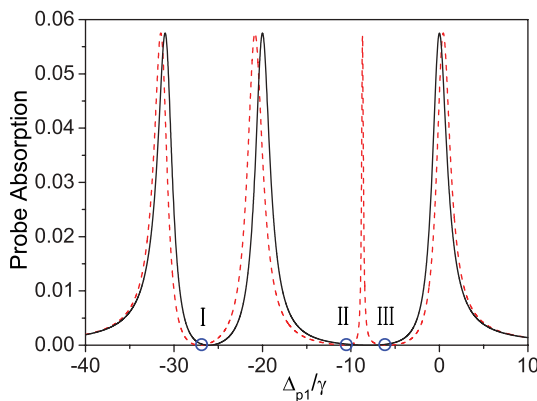
FIG. 3. (Color online) Probe absorption Im(χ) versus probe detuning Δ_{p1} at the SW nodes (black solid) and antinodes (red dashed) with all parameters the same as in Fig. 2.

the imaginary part of probe susceptibility χ is displayed as a function of the probe detuning Δ_{p1} at the SW nodes and antinodes, respectively. We find that the maximal SGC results in two transparency windows surrounded by three absorption lines at the SW nodes while the driving field splits them into three transparency windows surrounded by four absorption lines at the SW antinodes. Thus a FW propagating field will be reflected into a BW propagating field if most of its carrier frequencies fall into one transparency window of the cold atomic sample under consideration because the FW (BW) photons are exactly out of phase (in phase) during multiple Bragg scattering.

In particular, central positions of the three D-PBGs can be approximately determined by solving the interaction Hamiltonian in Eq. (1) to find three points of lowest probe absorption at the SW antinodes as denoted by the three blue circles in Fig. 3:

$$\Delta_{\rm I} = \frac{1}{9}\left(-A - 2\sqrt{C}\cos\frac{\theta}{3}\right),$$

$$\Delta_{\rm II} = \frac{1}{9}\left[-A + \sqrt{C}\left(\cos\frac{\theta}{3} + \sqrt{3}\sin\frac{\theta}{3}\right)\right], \quad (6)$$

$$\Delta_{\rm III} = \frac{1}{9}\left[-A + \sqrt{C}\left(\cos\frac{\theta}{3} - \sqrt{3}\sin\frac{\theta}{3}\right)\right],$$

with $A = 2(\omega_{21} + \omega_{31}) - 3\Delta_{s1}$, $B = \omega_{21}\omega_{31} - 2(\omega_{21} + \omega_{31})\Delta_{s1} - 8G_s^2$, $C = A^2 - 9B$, $D = AB + 27\omega_{31}(\omega_{21}\Delta_{s1} - 4G_s^2)$, and $\cos\theta = (A - 9D/2C)/\sqrt{C}$.

In Fig. 4, we plot probe absorption Im(χ) at the SW antinodes and probe reflectivity $|R|^2$ of the whole sample as a function of the dipole arrangement coefficient p with $\tilde{p} = 1.0$ for the frequency centers of D-PBGs I, II, and III, respectively. As we can see, when p gradually decreases from 1.0 to 0.0, the probe absorption (reflectivity) at the SW antinodes (of the whole sample) becomes larger and larger (smaller and smaller) so that all three D-PBGs are severely destroyed in the absence of SGC on the probe transitions. It is worth stressing that similar results can be observed (not shown) if we gradually decrease another dipole arrangement coefficient $\tilde{p}$ from 1.0 to 0.0 with $p = 1.0$. Thus both SGC on the triple probe transitions
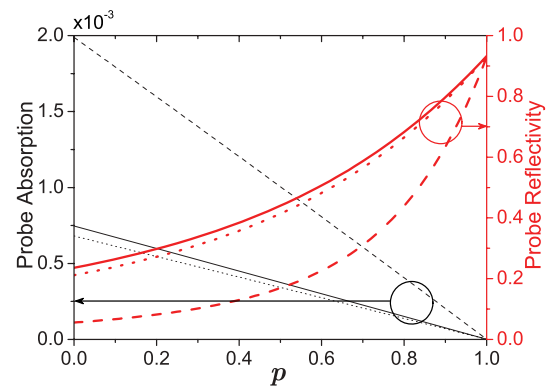
FIG. 4. (Color online) Probe absorption Im(χ) at the SW antinodes (thin black) and probe reflectivity $|R|^2$ of the whole sample (thick red) versus dipole arrangement coefficient p. Solid, dashed, and dotted curves correspond to centers $\Delta_{p1} = -26.6\gamma$, -10.2γ, and -6.6γ of D-PBGs I, II, and III, respectively. Other parameters are the same as in Fig. 2.
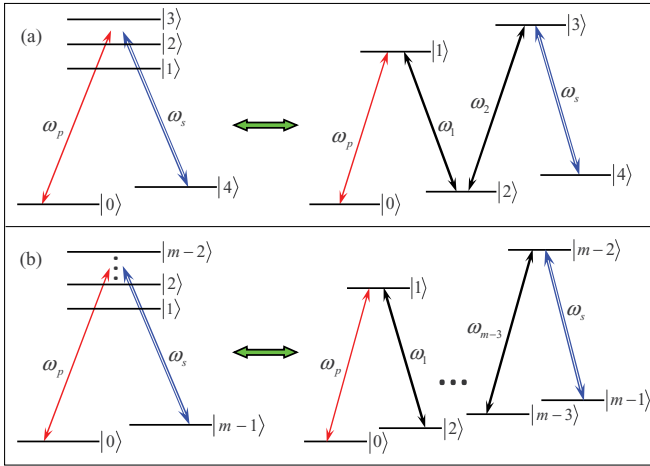
FIG. 5. (Color online) (a) A five-level triple-Λ system with SGC (left) and a five-level chain-Λ system without SGC (right). The latter is equivalent to the former in the dressed-state representation of two additional traveling-wave fields ω_1 and ω_2. (b) An m-level multi-Λ system with SGC (left) and an m-level chain-Λ system without SGC (right). The latter is equivalent to the former in the dressed-state representation of $m-3$ additional traveling-wave fields ω_1, ω_2, ..., ω_{m-3}.

and SGC on the triple driving transitions are essential for developing an ideal triple D-PBG structure around the probe resonance. The basic reason is that, with the dying down of p or $\tilde{p}$, the residual absorption becomes larger and larger within the three space-sensitive transparency windows, which then blurs all three D-PBGs [17].

It is worth noting that so far no real atoms or molecules are found to exhibit observable SGC due to the rigorous conditions of nearly degenerate levels and nonorthogonal dipole moments. Therefore the numerical results shown above seem impractical and useless as far as relevant experiments are concerned. Fortunately the triple D-PBGs can also be attained in a five-level chain-Λ system without SGC [the right one in Fig. 5(a)], which is equivalent to a five-level triple-Λ system with SGC [the left one in Fig. 5(a)] in the dressed state representation of two additional coupling fields ω_1 and ω_2. The five-level chain-Λ system, if described in the dressed state representation of ω_1 and ω_2, naturally satisfies the specific arrangement on dipole moments and field polarizations in the five-level triple-Λ system [cf. the last sentence in the paragraph just below Eq. (2)]. Accordingly, one may expect that $m-2$ D-PBGs will be simultaneously generated around the probe resonance in the case in which the five-level triple-Λ

(chain-Λ) system in Fig. 5(a) is extended into the m-level multi-Λ (chain-Λ) system in Fig. 5(d) with $m = 7, 9, 11, \ldots$.

To be more specific for potential experiments, we point out that a five-level chain-Λ system can be found on the D$_1$ line of cold ^{87}Rb atoms with the three lower levels referring to magnetic sublevels $|F = 2, m_F = -2\rangle$, $|F = 2, m_F = 0\rangle$, and $|F = 2, m_F = +2\rangle$ of the ground state $|5S_{1/2}\rangle$ and the two upper levels referring to magnetic sublevels $|F = 1, m_F = -1\rangle$ and $|F = 1, m_F = +1\rangle$ of the first excited state $|5P_{1/2}\rangle$. Similarly, one may find a seven-level (nine-level) chain-Λ system on the D$_1$ line of cold ^{85}Rb (^{133}Cs) atoms with the two hyperfine states $|5S_{1/2}, F = 3\rangle$ ($|6S_{1/2}, F = 4\rangle$) and $|5P_{1/2}, F = 2\rangle$ ($|6P_{1/2}, F = 3\rangle$) involved. In this case, the degeneracy of relevant magnetic sublevels should be broken by a static magnetic field of sufficient strength; the weak probe, TW coupling, and SW driving fields can be attained from a common laser passing through a series of acousto-optic modulators.

IV. CONCLUSIONS

In summary, we have shown that three D-PBGs can be simultaneously induced around the probe resonance by a SW driving field in a five-level triple-Λ system of cold atoms exhibiting SGC. The best developed triple D-PBG structure is attained when both SGC on the triple probe transitions and SGC on the triple driving transitions are maximal. If SGC is weakened on the probe or driving transitions, these D-PBGs will become remarkably malformed and even hardly defined as manifested by sufficiently reduced probe reflectivities due to increasing residual absorption. We also briefly mentioned the possibility of attaining three D-PBGs in a five-level chain-Λ system of cold atoms without SGC and the possibility of attaining more D-PBGs by suitably extending either one of the two five-level atomic systems. Clearly a multiple D-PBG structure is more appealing than a single or double D-PBG structure because it can be applied to synchronously manipulate more light signals of different frequencies in quantum networks, e.g., to devise tunable multichannel all-optical routing, switching, filtering, and reflectors even at the single-photon level.

[1] M. Fleischhauer, A. Imamoglu, and J. P. Marangos, Rev. Mod. Phys. **77**, 633 (2005).

[2] J. Mompart and R. Corbalan, J. Opt. B: Quantum Semiclass. Opt. **2**, R7 (2000).

[3] K. Bergmann, H. Theuer, and B. W. Shore, Rev. Mod. Phys. **70**, 1003 (1998).

[4] J. Appel, E. Figueroa, D. Korystov, M. Lobino, and A. I. Lvovsky, Phys. Rev. Lett. **100**, 093602 (2008).

[5] M. Bajcsy, A. S. Zibrov, and M. D. Lukin, Nature (London) **426**, 638 (2003).

[6] S. A. Moiseev and B. S. Ham, Phys. Rev. A **73**, 033812 (2006).

[7] K. R. Hansen and K. Molmer, Phys. Rev. A **75**, 053802 (2007).

[8] F. E. Zimmer, J. Otterbach, R. G. Unanyan, B. W. Shore, and M. Fleischhauer, Phys. Rev. A **77**, 063823 (2008).

[9] Y.-W. Lin, W.-T. Liao, T. Peters, H.-C. Chou, J.-S. Wang, H.-W. Cho, P.-C. Kuan, and I. A. Yu, Phys. Rev. Lett. **102**, 213601 (2009).

[10] J.-H. Wu, M. Artoni, and G. C. La Rocca, Phys. Rev. A **81**, 033822 (2010).

[11] J. Otterbach, J. Ruseckas, R. G. Unanyan, G. Juzeliunas, and M. Fleischhauer, Phys. Rev. Lett. **104**, 033903 (2010).

[12] A. Andre and M. D. Lukin, Phys. Rev. Lett. **89**, 143602 (2002).

[13] X. M. Su and B. S. Ham, Phys. Rev. A **71**, 013821 (2005).

[14] M. Artoni and G. C. La Rocca, Phys. Rev. Lett. **96**, 073905 (2006).

[15] S. M. Sadeghi, W. Li, X. Li, and W.-P. Huang, Phys. Rev. B **77**, 125313 (2008).

[16] C.-L. Cui, J.-H. Wu, J.-W. Gao, Y. Zhang, and N. Ba, Opt. Express **18**, 4538 (2010).

[17] J.-W. Gao, Y. Zhang, N. Ba, C.-L. Cui, and J.-H. Wu, Opt. Lett. **35**, 709 (2010).

[18] A. W. Brown and M. Xiao, Opt. Lett. **30**, 699 (2005).

[19] B. S. Ham, Appl. Phys. Lett. **88**, 121117 (2006).

[20] J.-H. Wu, M. Artoni, and G. C. La Rocca, Phys. Rev. Lett. **103**, 133601 (2009).

[21] J.-W. Gao, J.-H. Wu, N. Ba, C.-L. Cui, and X.-X. Tian, Phys. Rev. A **81**, 013804 (2010).

[22] S.-Y. Zhu and M. O. Scully, Phys. Rev. Lett. **76**, 388 (1996).

[23] C. H. Raymond Ooi, Phys. Rev. A **75**, 043818 (2007).

[24] X.-H. Yang and S.-Y. Zhu, Phys. Rev. A **77**, 063822 (2008).

[25] Y. Yang, J. Xu, H. Chen, and S.-Y. Zhu, Phys. Rev. Lett. **100**, 043601 (2008).

[26] V. Yannopapas, E. Paspalakis, and N. V. Vitanov, Phys. Rev. Lett. **103**, 063602 (2009).

[27] Z.-H. Li, D.-W. Wang, H. Zheng, S.-Y. Zhu, and M. S. Zubairy, Phys. Rev. A **82**, 050501(R) (2010).

[28] A. Joshi, W. Yang, and M. Xiao, Phys. Lett. A **325**, 30 (2004).

[29] A. Fountoulakis, A. F. Terzis, and E. Paspalakis, Phys. Rev. A **73**, 033811 (2006).

[30] M. Artoni, G. C. La Rocca, and F. Bassani, Phys. Rev. E **72**, 046604 (2005).